

# A Novel Dilute Antimony Channel In<sub>0.2</sub>Ga<sub>0.8</sub>AsSb/GaAs HEMT

Ke-Hua Su, Wei-Chou Hsu, *Member, IEEE*, Ching-Sung Lee, Tsung-Yeh Wu, Yue-Han Wu,  
Li Chang, Ru-Shang Hsiao, Jenn-Fang Chen, and Tung-Wei Chi

**Abstract**—This letter reports, for the first time, a high-electron mobility transistor (HEMT) using a dilute antimony In<sub>0.2</sub>Ga<sub>0.8</sub>AsSb channel, which is grown by a molecular-beam epitaxy system. The interfacial quality within the InGaAsSb/GaAs quantum well of the HEMT device was effectively improved by introducing the surfactantlike Sb atoms during the growth of the InGaAs layer. The improved heterostructural quality and electron transport properties have also been verified by various surface characterization techniques. In comparison, the proposed HEMT with (without) the incorporation of Sb atoms has demonstrated the maximum extrinsic transconductance  $g_{m,max}$  of 227 (180) mS/mm, a drain saturation current density  $I_{DSS}$  of 218 (170) mA/mm, a gate-voltage swing of 1.215 (1.15) V, a cutoff frequency  $f_T$  of 25 (20.6) GHz, and the maximum oscillation frequency  $f_{max}$  of 28.3 (25.6) GHz at 300 K with gate dimensions of  $1.2 \times 200 \mu\text{m}^2$ .

**Index Terms**—Dilute channel, InGaAsSb/GaAs high-electron mobility transistor (HEMT), surfactant.

## I. INTRODUCTION

THE OBJECTIVE of this letter is to investigate experimentally channel replacement in high-electron mobility transistor (HEMT) devices by incorporating Sb atoms during channel growth in order to improve the electrical properties of the two-dimensional (2-D) heterostructure. Dilute nitride [1] quaternary compounds In<sub>x</sub>Ga<sub>1-x</sub>As<sub>1-y</sub>N<sub>y</sub> have been intensively studied in the past few years [2], [3]. The InGaAsN/GaAs heterostructures possess the advantages of improving electron confinement at high temperatures due to their high conduction-band discontinuity barriers. In<sub>x</sub>Ga<sub>1-x</sub>As<sub>1-y</sub>N<sub>y</sub>, which may be strained or lattice-matched to the GaAs substrate, has been applied to 1.3- $\mu\text{m}$  laser diodes [4]–[6]. Besides, InGaAsN-based heterojunction bipolar transistors (HBTs) [7]–[9] have also demonstrated significant reductions in the turn-on voltages

as compared to the AlGaAs-based HBTs. The incorporation of N atoms can reduce the energy band gap, yet usually resulting in poor crystal qualities. Consequently, the N incorporation would seriously degrade the carrier transport [10], [11] for electronic device applications. In order to improve the optical property, annealing processes were attempted to remove the defects or the nonradiative impurities [6], [12], [13]. Recently, some efforts have been devoted to using Sb atoms as surfactants in the GaAs/InGaAsNSb quantum well (QW) laser to improve the crystal quality and to suppress 3-D growth [14]–[18]. The advantages of incorporating Sb atoms into the optoelectronic devices cannot only improve the threshold current densities [14]–[18] but also effectively reduce the energy band gap [19] and red-shift the light emission. Therefore, this letter presents, for the first time, a HEMT device using the dilute antimony In<sub>0.2</sub>Ga<sub>0.8</sub>AsSb channel grown by an MBE system to improve the interfacial quality, carrier transport properties, and channel-confinement capability at the same time. Enhanced device characteristics have been successfully achieved for the proposed InGaAsSb/GaAs HEMT, including improved carrier mobility, drain saturation current density, extrinsic transconductance, gate-voltage swing (GVS), and high-frequency characteristics, as compared to an identical InGaAs/GaAs HEMT structure without the Sb incorporation.

## II. MATERIAL GROWTH AND DEVICE FABRICATION

The epitaxial structure of the In<sub>0.2</sub>Ga<sub>0.8</sub>AsSb/GaAs HEMT was grown by the solid-source MBE system. The thermal cracked cells of arsenic and antimony were used as the group-V sources. The As flux was maintained constantly at about  $1 \times 10^{-6}$  torr during the entire growth procedure, and only the ratios between In and Ga were adjusted. An excess Sb flux of  $8 \times 10^{-8}$  torr, which was measured by the high-vacuum gauge, was introduced during the growth of the InGaAs channel by setting the cracked cell temperature at 550 °C for the Sb valve. The growth temperatures for the InGaAsSb and GaAs layers were set at about 510 °C and 600 °C, respectively. The epitaxial structure consists of a 0.4- $\mu\text{m}$  GaAs buffer layer on a (100)-oriented semi-insulating GaAs substrate, sequentially followed by a 9.5-nm In<sub>0.2</sub>Ga<sub>0.8</sub>AsSb channel, a 4-nm undoped GaAs spacer layer, a 20-nm Si-doped ( $5 \times 10^{18} \text{ cm}^{-3}$ ) GaAs carrier supply layer, a 15-nm undoped GaAs Schottky layer, and finally a 20-nm Si-doped ( $7 \times 10^{18} \text{ cm}^{-3}$ ) GaAs cap layer. An identical InGaAs/GaAs HEMT structure, except without incorporating the Sb atoms into the InGaAs channel, was also grown to provide direct comparison.

Manuscript received October 4, 2006; revised November 17, 2006. This work was supported by the National Science Council, Taiwan, R.O.C. under Contract NSC 94-2215-E-006-005. The review of this letter was arranged by Editor J. del Alamo.

K.-H. Su, W.-C. Hsu, and T.-Y. Wu are with the Advanced Optoelectronic Technology Center and the Institute of Microelectronics, Department of Electrical Engineering, National Cheng-Kung University, Tainan 70101, Taiwan, R.O.C. (e-mail: wchsuo@eembox.ncku.edu.tw).

C.-S. Lee is with the Department of Electronic Engineering, Feng Chia University, Taichung 40724, Taiwan, R.O.C.

Y.-H. Wu and L. Chang are with the Department of Materials and Engineering, National Chiao Tung University, Hsinchu 300, Taiwan, R.O.C.

R.-S. Hsiao and J.-F. Chen are with the Department of Electrophysics, National Chiao Tung University, Hsinchu 300, Taiwan, R.O.C.

T.-W. Chi is with the Industrial Technology Research Institute, Hsinchu 310, Taiwan, R.O.C.

Digital Object Identifier 10.1109/LED.2006.889047

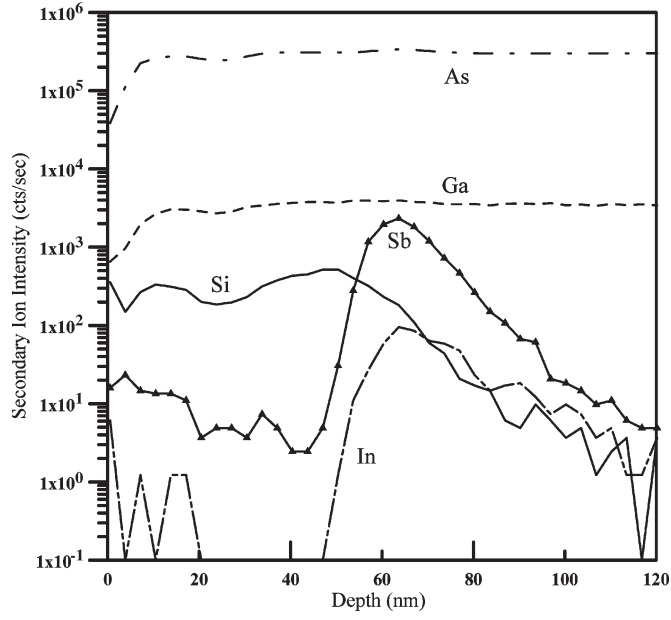


Fig. 1. SIMS measurement profiles for the InGaAsSb/GaAs HEMT.

Hall measurements were carried out on the proposed InGaAsSb/GaAs HEMT and the conventional InGaAs/GaAs HEMT samples to characterize the 2-D electron gas (2DEG) concentration  $n_{2\text{DEG}}$  and the electron mobility  $\mu_n$  under a magnetic field of 5000 G. The values of  $\mu_n$  and the corresponding  $n_{2\text{DEG}}$  were 2951 (2340)  $\text{cm}^2/\text{V}\cdot\text{s}$  and  $3.1(3) \times 10^{12} \text{ cm}^{-2}$  for the InGaAsSb (InGaAs)/GaAs HEMT at 300 K, respectively. Almost 26% improvement on the electron mobility with similar 2DEG concentrations has been observed and has verified the enhanced transport property by the Sb incorporation. Standard photolithography, lift-off, and rapid thermal annealing techniques were employed for the device fabrication. A AuGeNi alloy was used for the source-drain ohmic contacts, onto which Au was evaporated to reduce the contact resistance. Au was deposited on the undoped GaAs Schottky layer as the gate electrode. The gate dimensions were  $1.2 \times 200 \mu\text{m}^2$  with a drain-to-source spacing of  $7 \mu\text{m}$ . The mesa etching was performed down to the buffer layer to reduce the gate leakage current. The  $\text{H}_3\text{PO}_4/\text{H}_2\text{O}_2/\text{H}_2\text{O}$  solution was used as the wet-etching solution for the GaAs cap layer.

### III. EXPERIMENTAL RESULT AND DISCUSSION

Fig. 1 shows the secondary ion mass spectrometry (SIMS) intensity as a function of the junction depth of the InGaAsSb/GaAs HEMT. The InGaAsSb channel is inserted about 59 nm below the wafer surface. The Ga and As ions were both maintained with stable amounts during the sample growth, but both the In and Sb ion intensities were increased to their maximums at about 60 nm deep. The SIMS profiles demonstrated the successful incorporation of the Sb atoms within the channel growth. The Sb atoms reacted like surfactants to be slightly incorporated into the InGaAs film to improve the crystalline quality.

Fig. 2 shows the room-temperature photoluminescence (RT-PL) spectra for the InGaAsSb/GaAs and InGaAs/GaAs

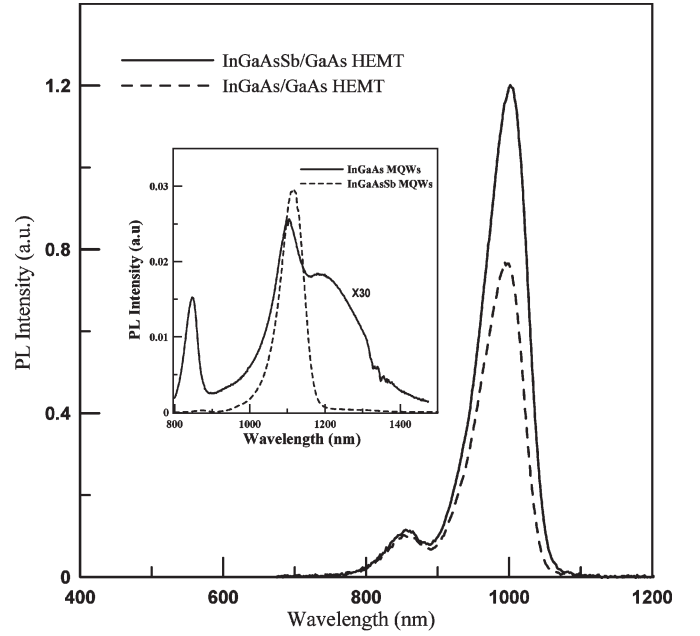


Fig. 2. RT-PL spectra for the InGaAsSb/GaAs and InGaAs/GaAs HEMTs, respectively. The inset shows PL characterizations for the  $\text{In}_{0.4}\text{Ga}_{0.6}\text{As}/\text{GaAs}$  MQW structures with/without the Sb incorporation.

HEMTs. The PL peak intensity of the InGaAsSb/GaAs HEMT increased by about 1.56 times as compared to that of the InGaAs/GaAs HEMT. The emission wavelength was shifted from  $0.993$  to  $1.002 \mu\text{m}$  due to the decreased energy band gap by the incorporation of Sb atoms. Both the PL intensity and the full-width at half-maximum (FWHM) clearly indicate the improved interfacial quality by adding the surfactantlike Sb atoms in the InGaAs channel. In addition, similar to the observation in the optoelectronic device [19], the incorporation of Sb atoms into the InGaAs compound can effectively decrease the energy band gap. This results in the improvements on both the electron transport property and the channel confinement capability as verified by the observed PL peak position. The PL characterization has shown consistent verification with the Hall measurement results, as discussed before. To further enhance the detectivity, the PL measurements were performed on the grown  $\text{In}_{0.4}\text{Ga}_{0.6}\text{As}/\text{GaAs}$  and  $\text{In}_{0.4}\text{Ga}_{0.6}\text{AsSb}/\text{GaAs}$  multiple quantum well (MQW) structures, respectively, as shown in the inset of Fig. 2. In order to distinguish the improvement in the heterostructural quality by the Sb incorporation, the In composition was increased to 0.4 in the MQWs to deliberately degrade the lattice mismatch within the InGaAs/GaAs heterostructure. The RT-PL spectrum of the InGaAsSb/GaAs MQW has shown more than 30 times brightness and a narrower FWHM of 73 nm than the 226 nm of the Sb-free structure. Clear improvement was observed by the Sb incorporation.

Fig. 3(a) and (b) show the TEM pictures for the InGaAs/GaAs and InGaAsSb/GaAs HEMTs, respectively. The InGaAsSb/GaAs interfaces within both the spacer/channel and channel/buffer heterostructures were observed to be more flat and uniform than the InGaAs/GaAs sample. The TEM photos also clearly demonstrate the improved crystal quality after the incorporation of Sb atoms.

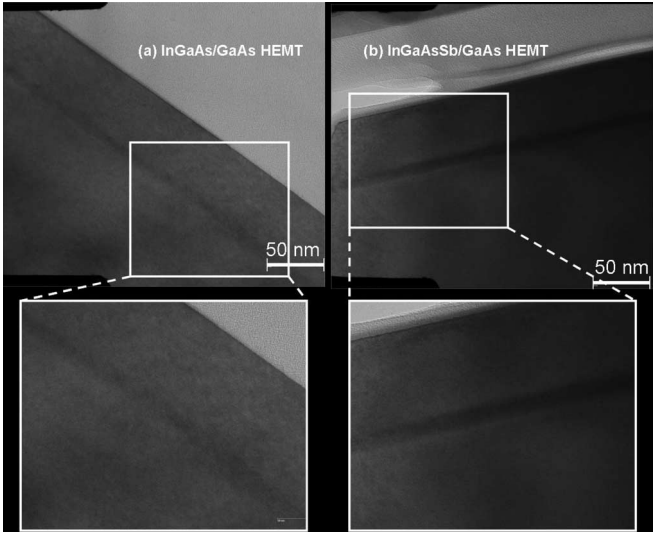


Fig. 3. TEM pictures of the (a) InGaAs/GaAs and (b) InGaAsSb/GaAs HEMTs.

Fig. 4(a) shows the typical current–voltage ( $I$ – $V$ ) characteristics of the InGaAsSb/GaAs HEMT and the conventional InGaAs/GaAs HEMT at 300 K, respectively. The drain–source saturation current densities  $I_{DSS}$ , which was defined at  $V_{GS} = 0$  V, are 208 and 171 mA/mm for the InGaAsSb/GaAs HEMT and the conventional InGaAs/GaAs HEMT, respectively. With comparable 2DEG concentrations as observed from the Hall measurement, the enhanced current drive capability of the present device is mainly attributed to the improved transport properties and the interfacial quality by adding the Sb atoms within the InGaAs QW channel. A possible reason for the observed lower  $I$ – $V$  slopes in the linear region of the InGaAsSb/GaAs sample than those of the InGaAs/GaAs sample is due to the control issue of the thermal evaporator system. Nevertheless, the InGaAsSb/GaAs sample did overcome the differences in contact resistance and demonstrated higher saturation current densities than the InGaAs/GaAs sample. This also proves that the transport property has been significantly enhanced at a high electric field due to the improved interfacial quality and carrier confinement by the Sb incorporation.

Fig. 4(b) indicates the  $g_{m,max}$  and  $I_{DSS}$  characteristics versus the applied gate–source bias for the studied InGaAsSb/GaAs and the conventional InGaAs/GaAs HEMTs at 300 K, respectively, with  $V_{DS} = 3$  V. The values of the  $g_{m,max}$  and the drain–source current density  $I_{DS}$  measured at  $V_{GS} = 2$  V are 227 (181) mS/mm and 473 (421) mA/mm at 300 K for the studied HEMT with (without) adding the Sb atoms into the InGaAs channel, respectively. A significant improvement of about 25% in the  $g_m$  value has been successfully achieved by employing the dilute antimony channel. With the GVS defined to be the available gate–source bias range at a drop of 10% from the  $g_{m,max}$  value, the proposed InGaAsSb/GaAs HEMT has demonstrated a wider GVS of 1.215 V ( $-0.715$  V  $\leq V_{GS} \leq 0.5$  V) than the 1.15 V ( $-0.75$  V  $\leq V_{GS} \leq 0.4$  V) of the conventional InGaAs/GaAs HEMT, as shown in Fig. 4(b). Possible reasons to account for the increased GVS are 1) the slight increase of the 2DEG concentration due to the decreased band gap in the InGaAsSb/GaAs QW [6], [12]–[15]

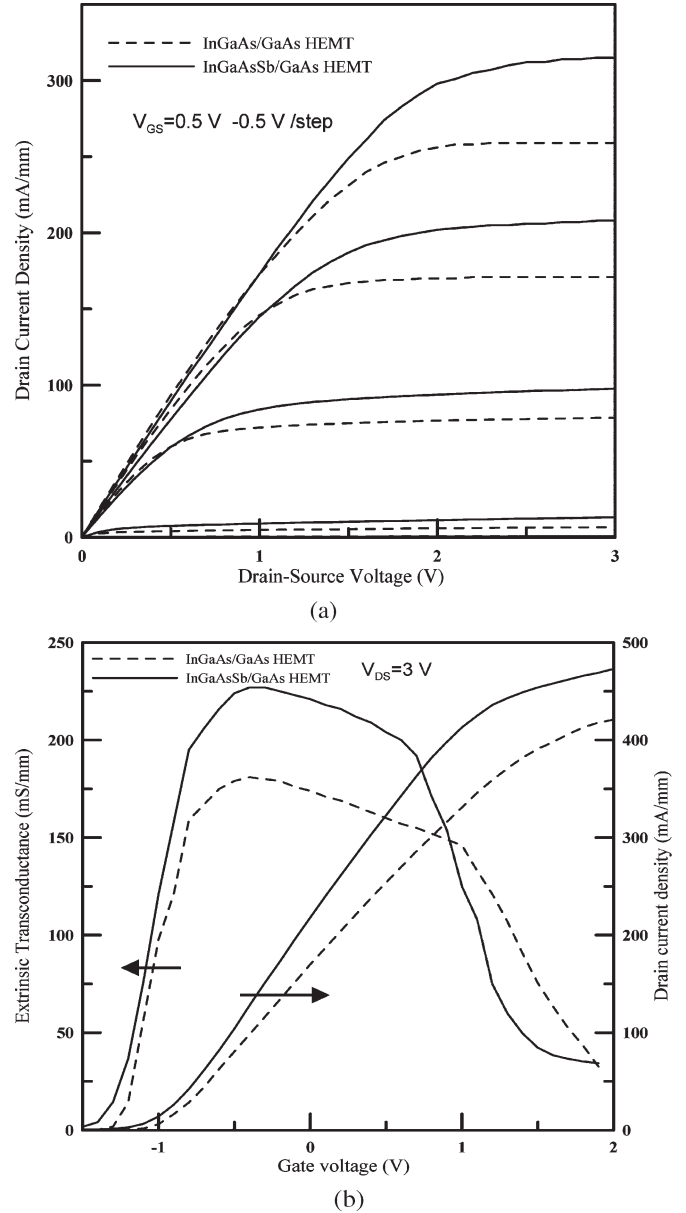


Fig. 4. (a) RT  $I$ – $V$  characteristics for the InGaAsSb/GaAs HEMT (solid line) and the InGaAs/GaAs HEMT (dotted line). (b)  $I_{DSS}$  and  $g_{m,max}$  characteristics versus  $V_{GS}$  at 300 K, with  $V_{DS} = 3$  V, for the InGaAsSb/GaAs HEMT (solid line) and the InGaAs/GaAs HEMT (dotted line).

and 2) the enhanced channel confinement capability due to the increased channel/buffer discontinuities to suppress the substrate leakages at higher channel potentials [16]. Thus, a more negative gate bias was required to deplete the carriers in the InGaAsSb channel. Consequently, improved device linearity with higher transconductance gain and enhanced current drive capability has been accomplished in the present InGaAsSb/GaAs device.

The microwave characteristics of the studied devices were characterized by using an HP8510B vector network analyzer in conjunction with the cascade probes over the range of 0.5–20 GHz. The gate dimensions were  $1.2 \times 200 \mu\text{m}^2$ . The unity gain cutoff frequency  $f_T$  and the maximum oscillation frequency  $f_{max}$  were determined to be 25 (20.6) and 28.3 (25.6) GHz at 300 K for the present HEMT with (without) the

dilute antimony channel, respectively, with  $V_{\text{DS}} = 2.5$  V and  $V_{\text{GS}} = -0.75$  V.

#### IV. CONCLUSION

A novel dilute antimony channel  $\text{In}_{0.2}\text{Ga}_{0.8}\text{AsSb}/\text{GaAs}$  HEMT grown on a GaAs substrate has been successfully investigated for the first time. Introducing the Sb atoms into the InGaAs channel to serve as surfactants can effectively improve the crystalline quality of the InGaAsSb/GaAs heterointerface. In addition, the decreased energy band gap of the dilute antimony channel can significantly improve the carrier transport properties and the channel confinement capability. Various characterization techniques, including SIMS spectrometry, PL spectra, Hall measurement, and TEM photography have been performed to verify the improvement. Consequently, superior device performances of high linearity, high extrinsic transconductance, and high current drive capability of the proposed InGaAsSb/GaAs HEMT have been successfully achieved in this letter.

#### REFERENCES

- [1] S. A. Choulis, T. J. C. Hosea, S. Ghosh, P. J. Klar, and M. Hofmann, "Postgrowth nondestructive characterization of dilute-nitride VCSELs using electroreflectance spectroscopy," *IEEE Photon. Technol. Lett.*, vol. 15, no. 8, pp. 1026–1028, Aug. 2003.
- [2] W. Shan, W. Walukiewicz, J. W. Ager, III, E. E. Haller, J. F. Geisz, D. J. Friedman, J. M. Olson, and S. R. Kurtz, "Band anticrossing in GaInNAs alloys," *Phys. Rev. Lett.*, vol. 82, no. 6, pp. 1221–1224, Feb. 1999.
- [3] K. Kim and A. Zunger, "Spatial correlations in GaInAsN Alloys and their effects on band-gap enhancement and electron localization," *Phys. Rev. Lett.*, vol. 86, no. 12, pp. 2609–2612, Mar. 2001.
- [4] K. D. Choquette, J. F. Klem, A. J. Fischer, O. Blum, A. A. Allerman, I. J. Fritz, S. R. Kurtz, W. G. Breiland, R. Sieg, K. M. Geib, J. W. Scott, and R. L. Naone, "Room temperature continuous wave InGaAsN quantum well vertical-cavity lasers emitting at  $1.3 \mu\text{m}$ ," *Electron. Lett.*, vol. 36, no. 16, pp. 1388–1390, Aug. 2000.
- [5] G. Steinle, F. Medere, M. Kicherer, R. Michalzik, G. Kristen, A. Y. Egorov, H. Riechert, H. D. Wolf, and K. J. Ebeling, "Data transmission up to 10 Gb/s with  $1.3 \mu\text{m}$  wavelength InGaAsN VCSELs," *Electron. Lett.*, vol. 37, no. 10, pp. 632–634, May 2001.
- [6] R. S. Hsiao, J. S. Wang, K. F. Lin, L. Wei, H. Y. Liu, C. Y. Liang, C. M. Lai, A. R. Kovsh, N. A. Maleev, J. Y. Chi, and J. F. Chen, "Single mode  $1.3 \mu\text{m}$  InGaAsN/GaAs quantum well vertical cavity surface emitting lasers grown by molecular beam epitaxy," *Jpn. J. Appl. Phys.*, vol. 43, no. 12A, pp. L1555–L1557, 2004.
- [7] P. C. Chang, A. G. Baca, N. Y. Li, X. Xie, H. Q. Hou, and E. Armour, "InGaP/InGaAsN/GaAs npn double heterojunction bipolar transistors," *Appl. Phys. Lett.*, vol. 76, no. 16, pp. 2262–2264, Apr. 2000.
- [8] P. C. Chang, N. Y. Li, C. Monier, A. G. Baca, J. R. LaRoche, H. Q. Hou, F. Ren, and S. J. Pearton, "Device characteristics of the GaAs/In-GaAsN/GaAs pnp double heterojunction bipolar transistor," *IEEE Electron Device Lett.*, vol. 22, no. 3, pp. 113–115, Mar. 2001.
- [9] C. Monier, A. G. Baca, P. C. Chang, N. Li, H. Q. Hou, F. Ren, and S. J. Pearton, "Pnp InGaAsN-based HBT with graded base doping," *Electron. Lett.*, vol. 37, no. 3, pp. 198–199, Feb. 2001.
- [10] A. J. Ptak, S. W. Johnston, S. Kurtz, D. J. Friedman, and W. K. Metzger, "A comparison of MBE- and MOCVD-grown GaInNAs," *J. Cryst. Growth*, vol. 251, no. 1, pp. 392–398, Apr. 2003.
- [11] J. F. Geisz, D. J. Friedman, J. M. Olson, S. R. Kurtz, and B. M. Keyes, "Photocurrent of 1 eV GaInNAs lattice-matched to GaAs," *J. Cryst. Growth*, vol. 195, no. 1–4, pp. 401–408, 1998.
- [12] J. S. Wang, A. R. Kovsh, R. S. Hsiao, L. P. Chen, J. F. Chen, T. S. Lay, and J. Y. Chi, "High nitrogen content InGaAsN/GaAs single quantum well for  $1.55 \mu\text{m}$  applications grown by molecular beam epitaxy," *J. Cryst. Growth*, vol. 262, no. 1–4, pp. 84–88, 2004.
- [13] A. R. Kovsh, J. S. Wang, L. Wei, R. S. Hsiao, J. Y. Chi, B. V. Volovik, A. F. Tsatsul'nikov, and V. M. Ustinov, "Molecular beam epitaxy growth of GaAsN layers with high luminescence efficiency," *J. Vac. Sci. Technol. B, Microelectron. Process. Phenom.*, vol. 20, no. 3, pp. 1158–1162, May 2002.
- [14] H. Shimizu, K. Kumada, S. Uchiyama, and A. Kasukawa, " $1.21 \mu\text{m}$  range GaInAs SOW lasers using Sb as surfactant," *Electron. Lett.*, vol. 36, no. 16, pp. 1379–1381, Aug. 2000.
- [15] X. Yang, M. J. Jurkovic, J. B. Heroux, and W. I. Wang, "Low threshold InGaAsN/GaAs single quantum well lasers grown by molecular beam epitaxy using Sb surfactant," *Electron. Lett.*, vol. 35, no. 13, pp. 1082–1083, Jun. 1999.
- [16] —, "Molecular beam epitaxial growth of InGaAsN:Sb/GaAs quantum wells for long-wavelength semiconductor lasers," *Appl. Phys. Lett.*, vol. 75, no. 2, pp. 178–180, Jul. 1999.
- [17] X. Yang, J. B. Heroux, L. F. Mei, and W. I. Wang, "InGaAsNSb/GaAs quantum wells for  $1.55 \mu\text{m}$  lasers grown by molecular-beam epitaxy," *Appl. Phys. Lett.*, vol. 78, no. 26, pp. 4068–4070, Jun. 2001.
- [18] W. Ha, V. Gambin, M. Wistey, S. Bank, H. Yuen, S. Kim, and J. S. Harris, Jr., "Long wavelength GaInAsSb/GaNAsSb multiple quantum well lasers," *Electron. Lett.*, vol. 38, no. 6, pp. 277–278, Mar. 2002.
- [19] H. Shimizu, K. Kumada, S. Uchiyama, and A. Kasukawa, "High-performance CW  $1.26 \mu\text{m}$  GaInAsSb-SQW ridge lasers," *IEEE J. Sel. Topics Quantum Electron.*, vol. 7, no. 2, pp. 355–364, Mar./Apr. 2001.